Journal of Advances in Science and Technology

Vol. IV, No. VII, November-2012, ISSN 2230-9659

REVIEW ARTICLE

INFLUENCE OF ELECTRONIC MEDIA ON THE READING HABITS OF PUPILS

www.ignited.in

Journal of Advances in Science and Technology
Vol. IV, No. VII, November-2012, ISSN 2230-9659

Influence of Electronic Media on the Reading Habits of Pupils

Rajbir

Research Scholar, CMJ University, Shillong, Meghalaya, India

----------♦----------

INTRODUCTION

The study of nuclear properties shows evidence of nuclear shells analogous to those observed in the atoms. One clear piece of evidence in the nuclear case is the sharp discontinuity in nucleon separation energies for certain numbers of N (neutron number) and Z (proton number), known as magic numbers. In the case of the electronic shells in atoms the picture is very clear, since there is a central Coulomb potential, due to the charge carried by the nucleus and electrons. In the case of the nucleus there is no such external potential but the nucleons move in the potential created by them selves. This potential contains many terms: central, spin-orbit, tensor, spinspin, etc. At long distances it has a Yukawa form , while at short distances it shows an extremely repulsive core. The idea of a shell model for the nucleus may seem contradictory with these strong correlations because this rudely breaks the independent particle picture.

We shall consider the nucleus as composed of Z protons and N neutrons, that interact via two-body forces and obey the Schr¨odinger equation, the general time independent form of which is ,

$$(- h^2 \Delta^2 / 2m + V) | \psi > = E | \psi \qquad (1.1)$$

where V is the potential and | i is the wave function with an associated energy E. The experimental idea of magic numbers led M. Goeppert-Mayer and H. Jensen to the construction of the nuclear mean field, a harmonic oscillator, whose main novelty was the very strong spin-orbit splitting needed to explain the experimental magic numbers. This idea originates from atomic physics in which the magnetic moment of an electron interacts with a magnetic field generated by its motion around the nucleus.

$$V(r) = ½ m w^2 r^2 + D l^2 - Cl.s \qquad (1.2)$$

where 1/2m?2r2 is the kinetic energy of an harmonic oscillator with frequency ? and mass m, l is the orbital angular momentum operator, s is the spin operator, D and C are constants to fit and where,

$$l.s = - ½ (j^2 – l^2 – s^2) = - ½ (j (j + 1) - l (l + 1) – ¾$$

$$= l + 1 \text{ for } j = l – ½$$

$$= - l \text{ for } j = l + ½ \qquad (1.3)$$

The single-particle levels of the nuclear mean field are represented in Fig. 1.1. The left-hand side shows the shell structure of the isotropic harmonic oscillator, then the splitting due to the l2 term and finally the single-particle levels taking into account the spin-orbit splitting. To the right are the predicted magic numbers. Therefore, due to the l.s term in the potential, the total degeneracy becomes (2j+1). This means that, for example, a 1p level, with a total degeneracy of 2(2l + 1) = 6, will split into two levels acording to Equation 1.3, 1p1/2 and 1p3/2 with degeneracies 2 and 4 respectively, see Fig. 1.1.

For a given nucleus (N,Z) the mean field dictates which levels are occupied (those below the Fermi level) and which are empty (those above). However, these states can be close enough in energy or have a structure such that the residual two body interaction can mix them to produce correlated states. Therefore, the infinite set of mean-field orbits will be divided in three parts:

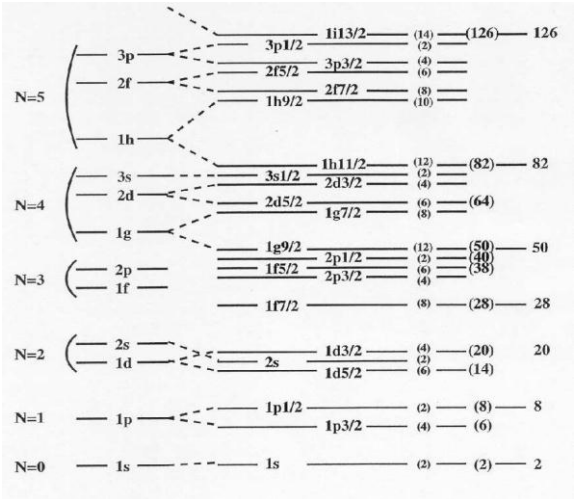

i) Inert core: the orbits that are forced to be always full. Imagine that the core consists of Nc neutrons and Zc protons, thus if we are studying a nucleus (N,Z) there will remain nv = N ? Nc valence neutrons and zv = Z ? Zc valence protons.

ii) Valence space: the orbits available to the valence particles, that will be partially occupied by them according to the effective interaction.

iii) External space: the remaining orbits that are always empty.

SAITAMA'S SHELLMODEL AND PAIR-TRUNCATED SHELLMODEL

This section focuses on the description of an effective shell model developed by the Saitama group (see Higashiyama et al.). In a shell model calculation it is necessary to include all the relevant orbits to describe a nucleus, but since this is not always feasible for medium-heavy nuclei, various truncation schemes are commonly used. To determine which orbitals should be included and make feasible the calculations, physical arguments are considered. The principal case of study of this thesis in terms of the shell model is 136 56Ba80 and the following considerations will be made for this nucleus. To truncate the model space, the proton single-particle orbitals involved in the calculations are restricted to the three orbitals. The neutron single-particle orbitals include all of the five orbitals between the N = 50 and 82 shell. The single-particle energies are extracted from experiment.

The effective shell-model hamiltonian is written as, H = Hv + $H_{\prod}$ + $Hv_{\prod}$, (1.4) where Hv + $H_{\prod}$ + $Hv_{\prod}$, represent the neutron interaction, the proton interaction and the neutron-proton interaction respectively. The interaction among like nucleons Hv + $H_{\prod}$ + $Hv_{\prod}$, consists of spherical single-particle energies, a monopole-pairing interaction (MP), a quadrupole-pairing interaction (QP), a quadrupole-quadrupole interaction (QQ), a hexadecapole-pairing (HP) and a hexadecapole-hexadecapole (HH) interaction. The strengths of these interactions are determined so as to reproduce the corresponding experimental energies of single-closed-shell nuclei. A detailed description of these interactions can be found in Ref. [4]. The definitions of the HP and HH interactions are extensions of the QP and the QQ interactions from angular momentum coupling two to four, but no radial dependence is assumed. The transition rates between levels are studied using the resultant shell-model wave functions.

NILSSON MODEL

In the Nilsson model the Schr¨odinger equation is solved using a deformed anisotropic harmonic oscillator potential that is parameterized with the deformation parameter β2. The Nilsson orbitals are defined with the following quantum numbers [N, nz,_], where is the projection of the angular momentum onto the symmetry axis, N is the total quantum number and determines the parity as (−1)N, nz is the number of oscillator shell quanta along the direction of the symmetry axis and _ is the projection of the particle orbital angular momentum l on the symmetry axis. In this deformed shell model the orbital angular momentum l and the intrinsic spin s are not conserved, i.e. they are not good quantum numbers.

BLOCKED BCS CALCULATIONS

In nuclei pairing correlations between nucleons are very important. The BCS model provides the theoretical basis to study these correlations in nuclei, in analogy to the Bardeen Cooper and Schrieffer (BCS) theory , which almost fifty years ago explained superconductivity in metals on the basis of electron pair correlations. There are clear analogies between both theories, for example if a superconductor is sufficiently heated, the Cooper pairs (correlated electrons) are broken and therefore the superconductivity is lost. In the case of a nucleus, if a nucleus is rotating sufficiently fast the pairing between nucleons is broken which manifests as an increase in the effective moment of inertia .

The pairing effect in the BCS theory is considered as a perturbation of the mean-field Hamiltonian and the solution of the eigenvalue problem is derived from a variational principle. The new states created are called single-quasiparticle states with energies given by,

$$E_k = ((E_k - \mu)^2 + \Delta^2)^{1/2} \qquad (1.11)$$

where ǫk is the single-particle energy for a Nilsson state k, μ is the Fermi energy and the pair gap, and G is the so called monopole pairing strength, which is one of the Hamiltonian parameters. The free parameter G is chosen in the BCS calculations to reproduce the lowest 2-quasiparticle states. The neutron pair strength Gv and a proton pair strength $G_{\prod}$ that are adjusted independently.

$$\Delta = G \sum v_k \mu_k \qquad (1.12)$$

The blocked BCS (BBCS) theory takes into account that the Nilsson level that has been occupied by an unpaired particle, cannot be occupied by another particle, and therefore the level is blocked. The Pauli principle prevents this level from participating in the scattering process of nucleons caused by the pairing correlations.The blocking effect manifests as a reduction in the pair gap.

$$\Delta = G \sum v_k \mu_k \qquad (1.13)$$

Where kj is the blocked orbital. This reduction in pairing energy can be large in some cases. This happens particularly for deformed nuclei where, although there are may be twenty or more single-particle levels in the spectrum, only four or five contribute appreciably to the sum .It can be taken

into account another residual interaction arising from the interaction of the intrinsic spins of the particles, the so called Gallagher and Moszkowski coupling rules . This interaction favours couplings of like particles with opposite spins and unlike particles with the same spin. Nevertheless the variation of the state energy will not change by more than a few hundred keV. A compilation of these residual interaction energies between proton-proton, neutron-neutron and proton-neutron orbitals in the 180 mass region can be found in Ref.

To carry out the BBCS calculations according to Ref. the deformation parameters β2 and β4, the proton (Z) and neutron (N) number and the neutron and proton pair strength Gv , G_{Π} are all required. The Nilsson single-particle energies ǫk, can be adjusted to reproduce the experimentally observed single-quasiparticle energies Ek in the neighbouring odd-mass nuclei. The pair gap, Δ, for each configuration of like particles is calculated by blocking the occupied orbitals. The multiquasiparticle energies, Emqp, are obtained by combining algebraically the neutron and proton configuration energies.

$$Em_{qp} = E^{v} + E^{\Pi} \qquad (1.14)$$

NEED OF THE STUDY

The different nuclear interactions between heavy ions can be, broadly speaking, divided into three main categories, depending on the energy involved in the interaction. Nevertheless, a nuclear reaction is determined in addition to the centre-of-mass energy by the impact parameter b and the nature of the projectile and target.

For low energy reactions (1-10 MeV/A) fusion evaporation type reactions might happen. These reactions occur at small values of the impact parameter and the projectile and target stay together for enough time (from 10−18 s to 10−16 s) to form a hot compound nucleus. In this case the resulting nuclei can be formed in a high spin state, thus allowing the nuclear spectroscopy of nuclear states at extremes of angular momentum. As the beam energy increases the reactions become more peripheral and the reaction times are much faster, ~ 10−22 s, and the impact parameter is extended compared to fusion-evaporation reactions. Nucleon transfer or deep inelastic reactions (DIC) can occur in which a few nucleons are transferred but the beam and target retain their original character. These reactions are still not completely understood as the mechanism through which nucleons are transferred becomes extremely complicated as the number of nucleons increases, but the study of these reactions provides valuable information on particle-particle correlations in nuclei, especially at energies close to the Coulomb barrier. In addition these reactions populate regions of the Segr´e Chart that otherwise can not be populated with fusion-evaporation reactions using stable beam and target combinations. For nearly a decade DIC have been successfully used to populate neutron rich nuclei for spectroscopic studies. During the last decade Broda et al. have used DIC with thick-targets and large arrays of germanium detectors to study exotic nuclei. It has been shown that using DIC it is possible to populate high-spin states in nuclei along the valley of stability and towards the neutron-rich side. For beam energies greater than about 40MeV/A a large fraction of the cross section goes into nuclear fragmentation, producing a large range of nuclei. The work carried out in this thesis involved the use of deep inelastic collisions and in the following sections these reactions are discussed in more detail.

DEEP-INELASTIC NUCLEAR REACTIONS

A considerable amount of data on deep inelastic collisions has been accumulated over the last three decades (e.g. [29, 30, 32, 40, 41]), albeit limited in character. From these accumulated experimental data, it is possible to list the following general features of DIC.

i) An essential feature is that these collisions preserve the binary character of the system, so that the final fragments maintain some resemblance to the initial nuclei,

ii) These reactions involve a fast redistribution of protons and neutrons among the colliding nuclei, which is governed by strong driving forces associated with the potential energy surface of the dinuclear complex. This fast rearrangement of neutrons and protons is called N/Z equilibration .The time involved in this equilibration is around 10−22 seconds .

iii) Momentum analyses of the nuclide distributions indicate that the exchange of nucleons starts out in an uncorrelated fashion . Then, due to the confinements imposed on the exchange process by the gradients of the potential energy surface,

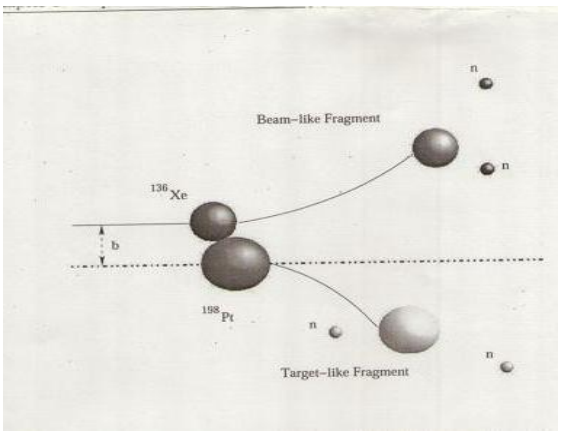

Semiclassical description of a Deep Inelastic Nuclear Reaction between heavy ions.

A correlation develops with increasing energy loss. Moreover, there are indications that the development of charge and mass flow is not only determined by macroscopic dynamics and liquid-drop potentials, but for small bombarding energies and small energy losses, single-particle degrees of freedom and tunneling probabilities add to the complexity of the observed phenomena .

iv) Angular momentum is transferred from relative orbital motion to the intrinsic spin of the two primary fragments

v) The primary fragments produced in these reactions de-excite mainly through the evaporation of light particles, namely neutrons, protons and α-particles, the emission of γ rays and in the case of heavier fragments via fission.

SCOPE OF THE STUDY

The heaviest β-stable platinum isotope, 198Pt, was used as a target for the reaction studied in this thesis to populate neutron-rich nuclei around mass 190. This nucleus was studied looking at both in-beam and out-of-beam γ-γ coincidences. The former allowed the study of the highest spins populated and the latter allowed the identification of a new high spin isomer.

Figure shows the level scheme for ^{198}Pt obtained by looking at γ-γ prompt coincidences. Some selected gates of the prompt Doppler corrected γ rays for ^{198}Pt are shown in Fig. All the levels for which spin-parity assignments are given in Fig., have been observed earlier , with the exception of the 802 and 813 keV transitions including the previously unreported 813 and 802 keV transitions. The widths of the arrows are proportional to the observed relative γ-ray intensity (black) and the electron conversion intensity (white).

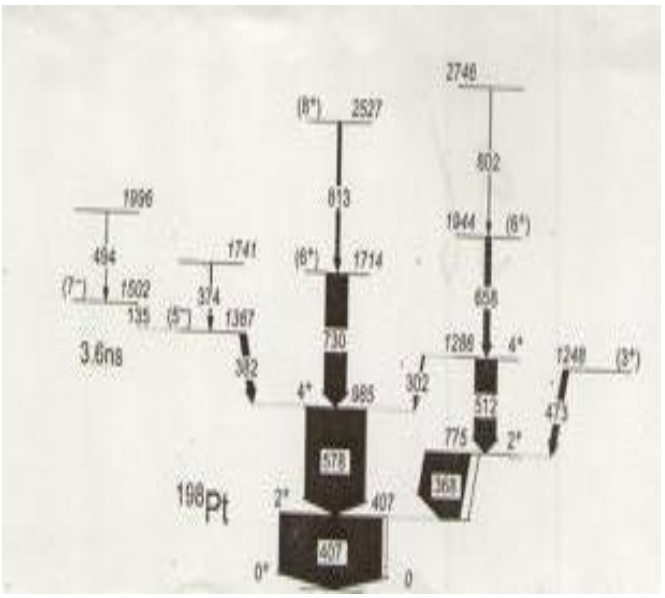

Level scheme of 198Pt, obtained by looking at prompt γ−γ coincidences,including the previously unreported 813 and 802 keV transitions. The widths of the arrows are proportional to the observed relative γ-ray intensity (black) and the electron conversion intensity (white).

Prior to this work the highest spin reported for 198Pt in the ground band was (6+) at 1714 keV excitation energy [137]. The spin and parity assignments for the 1714 keV level were deduced from the comparison of the experimental data with theoretical results obtained using the interacting boson model approximation and

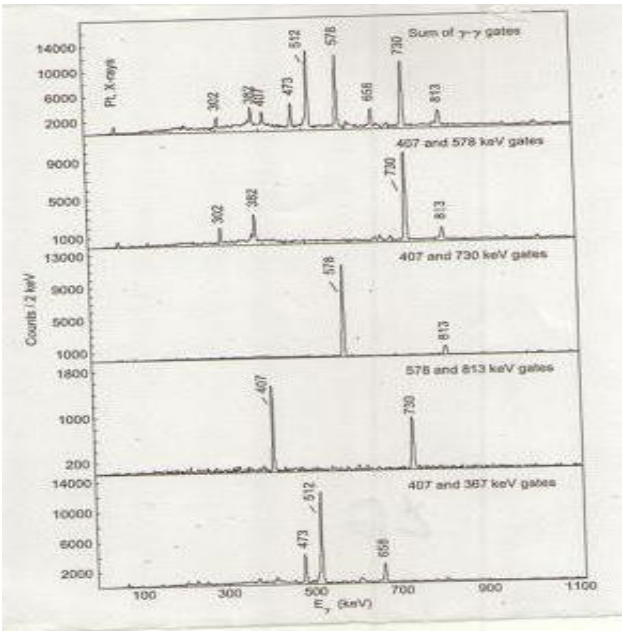

Figure : Background subtracted prompt γ-ray spectra for 198Pt. These spectra are sofware gated with a condition on the time range _t = ?45ns with respect to the detection of the recoils.

Systematics of the even platinum isotopes. In the current work the 813 keV transition has beenidentified to de-excite the proposed highest spin state identified, which has been assigned tentatively a spin-parity of (8+).

As in the case of ^{136}Ba some γ multipolarity information could be extracted for the prompt 813 keV transition, from the angular distribution. The A2 coefficient (the A4 coefficient is neglected in the fit), see Equation 1.34, for the 813 keV transition is 0.22±0.09, from which it can be concluded that it is a quadrupole transition within one standard deviation. The 2746 keV level decaying via a 802 keV γ-ray is reported for the first time in the current work and is observed to be in coincidence with the 658 and 512 keV transitions that belong to the γ band. Unfortunately, it was not possible to conclude anything about the multipolarity of the 802 keV prompt transition, from the study of the angular distributions. For the 658 keV transition, the A2 coefficient was found to be 0.23 ?0.09, which is in good agreement with a quadrupole transition within

one standard deviation. The energies and intensities of the prompt transitions observed are given in Table

E(keV)	Ei	E_f	$I_i^{[1]}$	$I_f^{[1]}$	I(delayed)
134.7	1502	1367	(7−)	(5−)	3(1)
301.5	1286	985	4+	4+	5(1)
367.6	775	407	2+	2+	136(5)
374.3	1741	1367		(5−)	4(1)
382.1	1367	985	(5−)	4+	21(2)
407.2	407	0	2+	0+	320(8)
473.4	1248	775	(3+)	2+	17(1)
494.0	1996	1502		(7−)	2(1)
511.7	1286	775	4+	2+	67(2)
577.9	985	407	4+	2+	185(6)
657.8	1944	1286	(6+)	4+	19(1)
729.5	1714	985	(6+)	4+	83(3)
801.8	2746	1944			2(1)
812.6	2527	1714	(8+)	(6+)	11(1)

ISOMERIC STATE IN ^{198}PT

Examining delayed γ−γ coincidences an isomer has been identified in ^{198}Pt. Figure shows all the transitions below the isomer, the known contaminants have been indicated next to the γ-ray transition energy. The 813 keV transition, decaying from the proposed (8+), can be clearly identified in Fig.

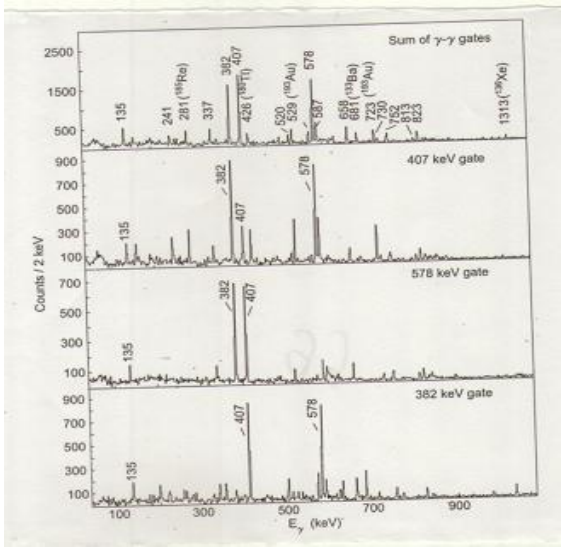

Figure : Background subtracted delayed γ-ray spectra for 198Pt. The time condition is that the γ rays are observed in the time range _t = 30 − 150 ns with respect to the detection of the two binary fragments.

The time condition is that the γ rays are observed in the time range Δt = 30 − 150 ns with respect to the detection of the two binary fragments.

OBJECTIVES OF THE STUDY

In a binary reaction, the γ rays detected in each event can come from one or both of the fragments and a priori, there is no way to assign a γ ray to a specific fragment. In the case of prompt γ rays it is possible to distinguish whether the γ ray comes from TLFs or BLFs. Therefore it is possible to study the distribution of the binary partners using delayed-prompt coincidences. An isomer in one of the binary partners and prompt feeding in the other is needed, a situation which is quite likely for the region of nuclei populated in the reaction studied. Here the way to proceed is to gate on delayed γ-ray transitions from well-known isomers and project the prompt γ rays from the binary fragment. For this purpose a delayed-prompt matrix was produced, where the prompt γ rays are Doppler corrected for TLFs.

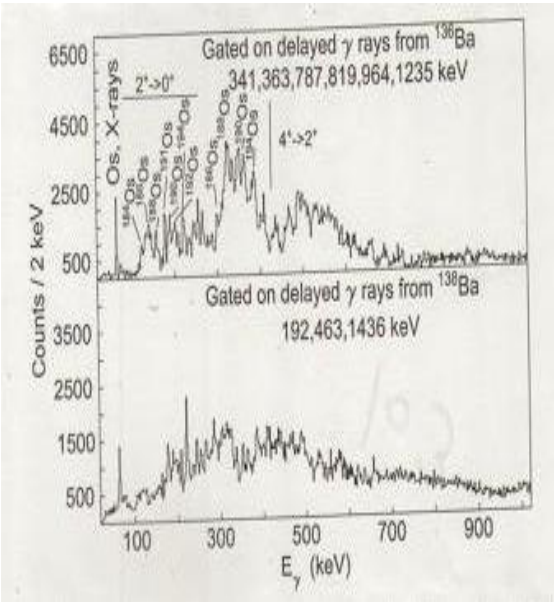

Figure: Background subtracted prompt γ-ray spectra for osmium isotopes, gated on delayed barium γ rays. The upper panel is gated by 138Ba delayed γ rays, whose binary partner is 196Os and the lower panel is gated by 136Ba delayed γ rays, whose binary partner is 198Os.

.Figure shows background subtracted prompt γ-ray spectra for osmium isotopes, gated on the delayed γ rays of the barium binary partner. The delayed gates have been chosen carefully, so that there is no

contamination from other nuclei at these energies. The osmium X-rays are clearly visible in the spectra and there are no other obvious X-ray lines from other nuclei . Therefore the gates taken to create the spectra are clean and it is mainly prompt Doppler corrected osmium γ rays which are projected. The large background in the spectra is due to delayed γ rays that have been Doppler corrected with the incorrect β value and are thus smeared out.

Figure shows background subtracted prompt γ-ray spectra for platinum isotopes, gated on delayed γ rays of the xenon binary partner. The platinum X-rays are clearly visible in all the spectra. The upper spectrum is very clean in terms of the platinum isotopes, where the most prominent peak is the 2+ → 0+ transition from the target nucleus, ^{198}Pt.

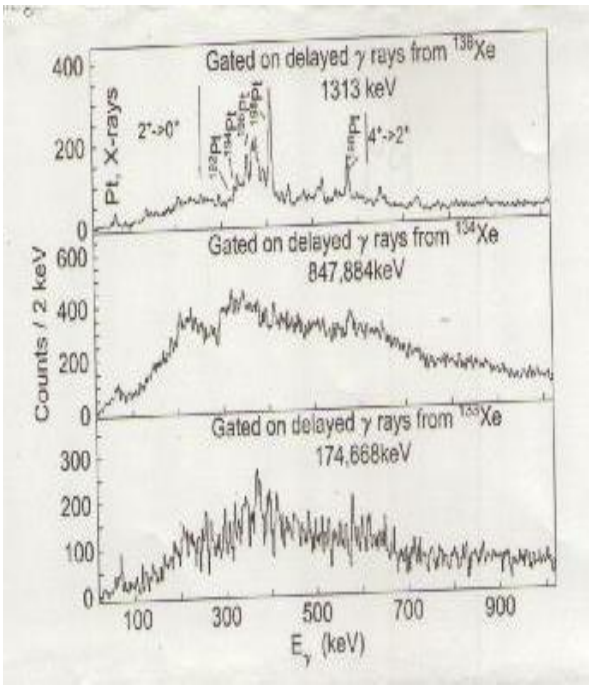

Background subtracted prompt γ-ray spectra for platinum isotopes, gated by delayed xenon γ rays. The upper panel is gated by ^{136}Xe delayed γ rays, whose binary partner is ^{198}Pt. The middle panel is gated by ^{134}Xe delayed γ rays, whose binary partner is ^{200}Pt and the lower panel is gated by ^{133}Xe delayed γ rays, whose binary partner is ^{201}Pt. Note that xenon and platinum are binary partners.

Figures show characteristic γ rays from a range of osmium and platinum isotopes respectively. The intensity of each of these γ rays is, a priori, related to the probability of neutron evaporation from the hot binary fragment produced after the reaction. This can be quantified using the Relative Yield parameter, calculated using the efficiency and internal conversion corrected intensity of the 2+ → 0+ γ ray for each even-even osmium isotope. In the case of 191Os the intensity of the 11/2+ → 9/2−, E1 γ ray has been used. Each value has been normalized such that the Relative Yield for the 194Os isotope has a value of 10.

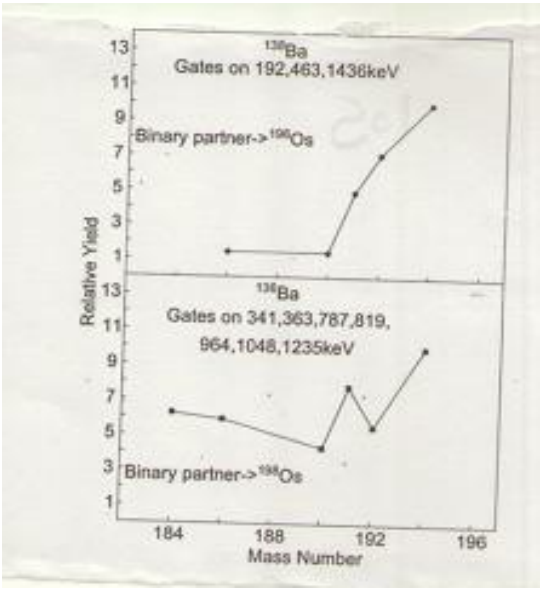

The upper panel shows the Relative Yield for osmium isotopes gated by 138Ba, whose binary partner is 196Os which is unknown. The lower panel shows the Relative Yield for osmium isotopes gated on ^{136}Ba, whose binary partner is ^{198}Os.

The study of the Relative Yield parameter was used first in fission experiments to study the isotopes produced in the fission process and to identify the isotopes of interest. Figure shows the Relative Yield for different osmium isotopes, ranging from 184Os to 194Os, gated on delayed γ rays from ^{138}Ba (upper panel) and ^{136}Ba (lower panel). The plots show the maximum yield for 194Os. Unfortunately heavier osmium isotopes could not be investigated, since their γ ray transitions are not known in the literature. If heavier isotopes could be identified a peak would be expected centred on the most populated isotope. In this manner one could determine the most likely number of evaporated neutrons. The Relative Yield calculated should not be taken as strictly defined probabilities of neutron evaporation of the excited fragments, since most of these osmium isotopes, for example 190Os, 191Os, 192Os and 194Os, have isomers. Therefore the intensity trapped in these isomers, which is not known, reduces the Relative Yield, thus biasing the results. It could be possible to do the same Relative Yield analysis for the platinum isotopes. However, in this case the Yield due to Coulomb scattering for the ^{198}Pt isotope should be included. In addition, some of the platinum isotopes have isomers (e.g. ^{192}Pt and ^{198}Pt), therefore detailed information on the average neutron evaporation could not be extracted, clearly in the current work.

196OS OR NOT 196OS, THAT IS THE QUESTION.

Figure shows a strong transition at 283 keV from one of the osmium isotopes. This energy happens to be in the energy range expected for the 2+ → 0+ transition for ^{196}Os, which was measured to be 300 ?20keV [144], and it might be expected in this spectrum. The 196Os isotope was previously studied

via two proton pickup on ^{198}Pt , using the reaction ^{198}Pt(^{14}C,^{16}O)^{196}Os.

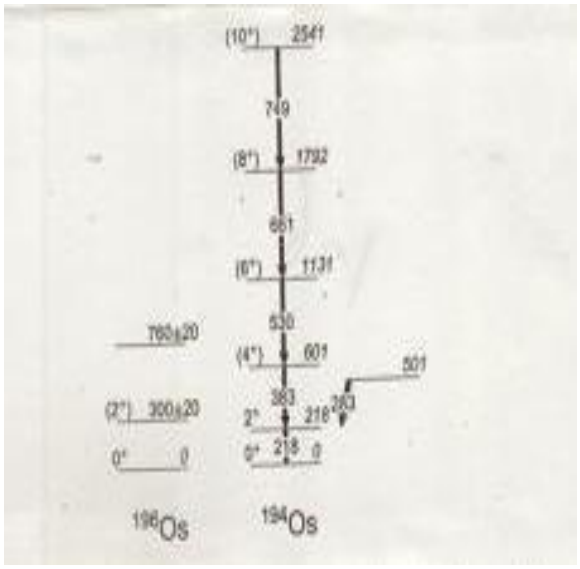

Level scheme of ^{196}Os, taken from (left) and level scheme for ^{194}Os, including the new 283 keV transition deduced from the present work (right).

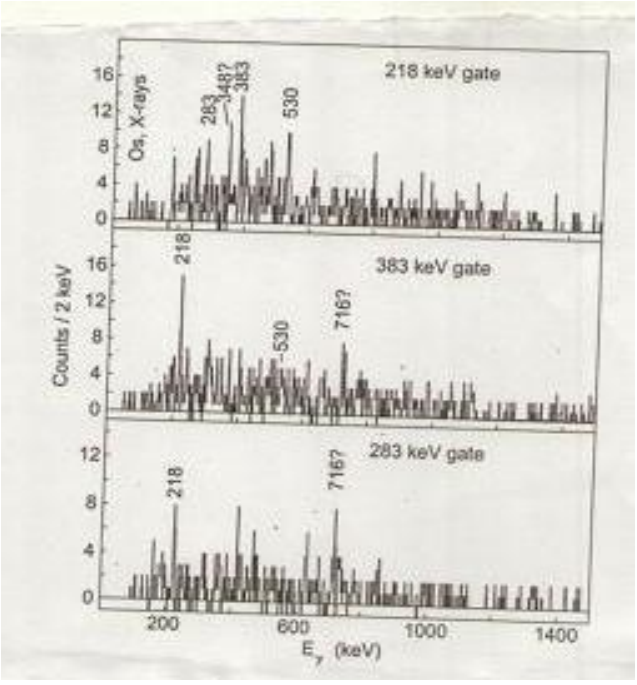

Background subtracted prompt γ-ray spectra for 194Os. These spectra have been obtained by looking at γ-γ prompt coincidences. The γ-γ prompt matrix has been gated on the delayed 192, 463 and 1436 keV γ rays from the binary partner ^{138}Ba.

A delayed-prompt-prompt cube, where the prompt γ rays are Doppler corrected for TLFs (see Table), was produced to elucidate whether the 283 keV transition corresponds to the 2+ → 0+ transition in 196Os. Figure shows background subtracted prompt γ-ray spectra gated on the delayed 192, 463 and 1436 keV γ rays from the binary fragment 138Ba. The top panel in Fig. shows the γ-ray spectra gated on the prompt 218 keV, 2+ → 0+ transition in 194Os and shows the

383 keV 4+ → 2+, the 530 keV 6+ → 4+ and the unplaced 283 keV transitions. The middle panel of the former figure shows the γ-ray spectra gated on the prompt 383 keV, 4+ → 2+ transition in 194Os which shows the 218 keV 2+ → 0+ and the 530 keV 6+ → 4+ transitions but not the unplaced 283 keV transition. The lower panel shows the γ-ray spectra gated on the prompt unplaced 283 keV transition. This gate is in coincidence with the 218 keV transition from 194Os. Therefore the conclusion is that the 283 keV transition probably belongs to 194Os and not to 196Os.

The final level scheme for 194Os deduced in the current work can be seen in Fig . Figure shows γ rays at energies 348 and 716 keV that due to lack of statistics could not be placed in the current level scheme. The highest spin state observed in the current work for 194Os is the (10+) 2541 keV state, previously reported by Wheldon et al. [145]. This state has been found to be isomeric in the current work and an upper limit to the half-life has been obtained namely t1/2 < 90ns.

BIBLIOGRAPHY

[1] A. Messiah, Quantum Mechanics, North-Holland, Amsterdam (1965).

[2] M.G. Mayer et al., Phys. Rev. 75, 1969 (1949).

[3] A. Poves and F. Nowacki, Lecture Notes in Physics, Springer, (2001).

[4] K. Higashiyama, N. Yoshinaga and K. Tanabe, Phys. Rev. C 65, 054317 (2002).

[5] K. Higashiyama, N. Yoshinaga and K. Tanabe, Phys. Rev. C 67, 044305 (2003).

[6] F. Iachello and A. Arima, Phys. Lett. B 53, 309 (1974).

[7] R.F. Casten, Nuclear Structure from a Simple Perspective, Oxford Science Publications 2000.

[8] J.J. Ressler et al., Phys. Rev. Lett., submitted (2003).

[9] M. Eisenberg and W. Greiner, Microscopic Theory of the Nucleus, North- Holland Publishing Company (1972).

[10] W. Greiner, Nuclear Models, Springer-Verlag Berlin Heidelberg New York (1996).

[11] S.G. Nilsson, Dan. Mat.-Fys. Medd. 29, 16 (1995).

[12] J. Bardeen, L.N. Cooper and J.R. Schrieffer, Phys. Rev. 108, 1175 (1957).